

RESEARCH ARTICLE

Editorial Process: Submission:02/12/2022 Acceptance:03/08/2023

The Role of Pre-Operative MRI for Prediction of High-Grade Intracranial Meningioma: A Retrospective Study

Kan Radeesri, Vitit Lekhavat*

Abstract

Objective: High histological grade (WHO grade 2 and 3) intracranial meningiomas have been linked to a greater risk for tumor recurrence and worse clinical outcomes compared to low-grade (WHO grade 1) tumors. Preoperative magnetic resonance imaging (MRI) plays a crucial role in tumor evaluation and allows a better understanding of tumor grading, which could potentially alter clinical outcomes. The present study sought to determine whether preoperative MRI features of intracranial meningiomas can serve as predictors of high-grade tumors. **Methods:** This retrospective study reviewed 327 consecutive confirmed cases of intracranial meningiomas, among whom 210 (64.2%) had available preoperative MRI studies. Thereafter, imaging features such as intratumoral signal heterogeneity, venous sinus invasion, necrosis or hemorrhage, mass effect, cystic component, bone invasion, hyperostosis, spiculation, heterogeneous tumor enhancement, capsular enhancement, restricted diffusion, brain edema, and unclear tumor-brain interface were obtained and data were analyzed using univariate and multivariate analyses. **Results:** 249 (76.1%) patients had low-grade (grade I), and 78 (23.9%) had high-grade (grades 2 and 3) intracranial meningioma. The majority of cases were females (274 cases, 83.3%) and most patients were below 60 years of age (mean age, 52.50 ± 11.51 years). The multivariate analysis with Multiple Logistic regression analysis using factors determined to be significant during univariate analysis via a backward stepwise selection method with statistical significance set at 0.05 identified three MRI features including necrosis or hemorrhage (adjusted OR = 2.94, 95% CI: 1.15–7.48, $p = 0.024$), hyperostosis (adjusted OR = 0.31, 95% CI: 0.12–0.79, $p = 0.014$), and brain edema (adjusted OR = 2.33, 95% CI: 1.13–4.81, $p = 0.022$) as significant independent predictors of high-grade meningioma after adjusting for confounders. **Conclusions:** Our study suggested that certain preoperative MRI features of intracranial meningiomas including necrosis or hemorrhage and brain edema could potentially predict high-grade tumors while hyperostosis is a predictor for low-grade tumors.

Keywords: Meningioma- high-grade- WHO histological grading- preoperative MRI- predictive factor- MeSH

Asian Pac J Cancer Prev, 24 (3), 819-825

Introduction

Meningiomas originate from meningotheelial cells, otherwise known as the arachnoid cap, and are the most prevalent non-glial primary brain tumors. The current WHO classification of brain tumors classifies meningiomas into three categories: common (WHO grade 1), atypical (grade 2), and anaplastic or malignant (grade 3) (O'leary et al., 2007; Louis et al., 2021). WHO Grade I meningiomas are generally considered benign with a low risk of recurrence. Atypical meningiomas (WHO Grade 2), which account for 20%–35% of all meningiomas, exhibit recurrence rates of up to 50% and 10-year survival rates of <80% (Budohoski et al., 2018). Anaplastic meningiomas (WHO Grade 3) are rare, accounting for only 3% of all meningiomas, with a recurrence rate of up to 94% and low overall survival rates (Claus et al., 2005). The extent of surgical resection and histological type of meningioma

have both been considered as prognostic factors for tumor recurrence (Ogasawara et al., 2021). Available evidence suggests that preoperative tumor grades can influence patient treatment strategies, with those having more aggressive (WHO grade 2/3) meningiomas potentially benefiting from early and complete resection (Rogers et al., 2015; Goldbrunner et al., 2016; Hwang et al., 2016; Hale et al., 2018). Magnetic resonance imaging (MRI) plays a crucial role in detecting lesions, evaluating tumor-related complications, and establishing presurgical differential diagnoses of intracranial meningiomas given its excellent soft tissue resolution and multiplanar capabilities (O'leary et al., 2007). Moreover, imaging features of a typical meningioma enable precise and reliable diagnosis in the majority of cases (Watts et al., 2014). However, it remains unclear whether classic MRI features of meningioma, such as signal characteristics on T1- and T2-weighted images and a dural tail appearance,

can predict higher histological grades (Gurkanlar et al., 2005; Hsu et al., 2008; Lee et al., 2008). Furthermore, certain meningiomas may exhibit atypical imaging characteristics in terms of signal intensity, tumor location, and behavior, which may not always indicate atypical histology (O'leary et al., 2007). Several prior studies have suggested a relationship between MRI features and histological high-grade meningiomas, such as the presence of tumor necrosis/hemorrhage, indistinct tumor–brain interface, heterogeneous tumor enhancement, and peritumoral brain edema (Kawahara et al., 2012; Lin et al., 2014; Coroller et al., 2017; Hale et al., 2018). The current study aimed to determine whether preoperative MRI features of intracranial meningioma can serve as predictors of high-grade histological tumor grading using univariate and multivariate statistical analyses in a relatively large number of pathologically confirmed patients.

Materials and Methods

Patients

The current study was approved by the Bioethics Committee of Navamindradhiraj University (COA 173/63). The inclusion criteria include patients who were initially diagnosed with and underwent resection for intracranial meningioma at Vajira hospital, a tertiary care university hospital, between 2013 and September 2020. A total of 327 consecutive patients with histologically confirmed intracranial meningioma were identified. Variables were then collected from provider notes, pathology records, operative notes, and radiological reports. The exclusion criteria include patients with recurrent disease and preoperative MRI could not be interpreted. The need for informed consent was waived given the retrospective study design.

MRI analysis

MRI was performed with a similar protocol by either 1.5 Tesla Philips Achieva or 3.0 Tesla Philips Ingenia. The MRI protocol includes T1-weighted (T1W), T2-weighted (T2W), Fluid inversion recovery (FLAIR), diffusion-weighted imaging (DWI), susceptibility-weighted imaging (SWI), and gradient echo (GRE). All patients received intravenous gadolinium contrast. Imaging features of the cases that had available preoperative MRI findings were independently reviewed by two neuroradiologists (V.L. and K.R.) with 9-year of experience who were blinded to clinical history or pathologic grade and disagreement was resolved by consensus. MR images were evaluated for tumor location and presence of other imaging features, including intratumoral signal heterogeneity (determined by subjective evaluation of intratumoral signal on T1W or T2W), peritumoral brain edema (Figure 1A and B) which was determined by the presence of high signal intensity on T2W or FLAIR adjacent to the tumor, multifocality, midline shift, venous sinus invasion, necrosis (determined by the presence of non-enhancing area within the tumor/hemorrhage (determined by the presence of blooming artifacts on SWI or GRE (Figure 2A and B), mass effect (determined by the presence of pressure effect to any adjacent intracranial structures), cystic

component (defined as fluid signal seen on T2W), bone invasion, hyperostosis, spiculation, heterogeneous tumor enhancement (Fig. 1B), capsular enhancement (defined as rim-enhancing seen on post gadolinium images), and restricted diffusion. The tumor–brain interface was categorized as “clear” or “unclear,” in which tumors with a distinct low-intensity border and obvious demarcation from the brain or edema were regarded as “clear,” whereas those without a distinct border were regarded as “unclear.” Tumor location was grouped in the following categories: skull base, parafalcine/parasagittal, convexity, posterior fossa, and cavernous.

Statistical analysis

Univariate and multivariate analyses were performed to determine potential preoperative MRI features that could predict high-grade meningiomas. Results of Multiple Logistic regression analyses were presented as odds ratios with 95% confidence intervals reflecting the odds of high-grade meningioma. For univariate analysis, independent samples t-test, Chi-square test, or Fisher's exact test were performed to investigate the association between the clinical characteristics, including gender, age, and preoperative MRI features. All statistical analyses were performed using IBM SPSS Statistics for Windows, version 26.0.

Results

The final study cohort included 327 patients, among whom 249 (76.1%) and 78 (23.9%) had low-grade (grade I) and high-grade (grades 2 and 3) intracranial meningioma, respectively. Females accounted for the majority of the overall cases (274 cases, 83.3%). Female predominance was also found in both the low- and high-grade intracranial meningioma groups (87.6% and 71.8%, respectively; Table 1). Most patients were below 60 years of age upon diagnosis (mean age, 52.50 ± 11.51 years; Table 1).

Among the 327 patients, 210 (64.2%) had available preoperative MRI studies. No significant differences were found between patients with high- and low-grade intracranial meningioma, among whom 50 (64.1%) and 160 (64.3%) had available preoperative MRI studies, respectively (Table 1). Skull base was the most common location for intracranial meningioma (86 cases, 41%). The percentages of other locations are detailed in Table 1. Comparison of the MRI findings in patients with high- and low-grade intracranial meningioma found that intratumoral signal heterogeneity (p-value 0.010), midline shift (p-value 0.025), necrosis or hemorrhage (p-value 0.001), heterogeneous tumor enhancement (p-value 0.002), restricted diffusion (p-value 0.011), and brain edema (p-value 0.003) were observed more in high-grade meningioma while hyperostosis has seen more in low-grade group (Table 2). Univariate analysis with Binary Logistic regression analysis identified male sex (OR = 2.84, 95% CI: 1.33–6.06, p value = 0.007), parafalcine/parasagittal (OR = 3.79, 95% CI: 1.54–9.33, p = 0.004), intratumoral signal heterogeneity (OR = 2.30, 95% CI: 1.21–4.39, p = 0.011), midline shift (OR = 2.08,

Table 1. General and Clinicoradiological Characteristics of the Patients

| Characteristics | Total | Low-Grade | High-Grade | p-value |
|--------------------------|---------------|---------------|---------------|---------|
| No. of patients | 327 (100.0) | 249 (76.1) | 78 (23.9) | - |
| Sex | | | | |
| Male | 53 (16.2) | 31 (12.4) | 22 (28.2) | 0.001 |
| Female | 274 (83.8) | 218 (87.6) | 56 (71.8) | |
| Age (years) | 52.50 ± 11.51 | 52.14 ± 11.18 | 53.65 ± 12.50 | 0.312 |
| <60 | 241 (73.7) | 187 (75.1) | 54 (69.2) | 0.304 |
| ≥60 | 86 (26.3) | 62 (24.9) | 24 (30.8) | |
| Preoperative MRI | | | | |
| Yes | 210 (64.2) | 160 (64.3) | 50 (64.1) | 0.98 |
| No | 117 (35.8) | 89 (35.7) | 28 (35.9) | |
| Location | | | | |
| Skull base | 86 (41.0) | 69 (43.1) | 17 (34.0) | 0.036 |
| Parafalcine/parasagittal | 29 (13.8) | 15 (9.4) | 14 (28.0) | |
| Convexity | 28 (13.3) | 22 (13.8) | 6 (12.0) | |
| Posterior fossa | 29 (13.8) | 22 (13.8) | 7 (14.0) | |
| Cavernous sinus | 10 (4.8) | 8 (5.0) | 2 (4.0) | |
| Multicompartment | 28 (13.3) | 24 (15.0) | 4 (8.0) | |

Data are presented as number (%) or mean ± standard deviation; The p value corresponds to independent samples t-test, Chi-square test, or Fisher's exact test.

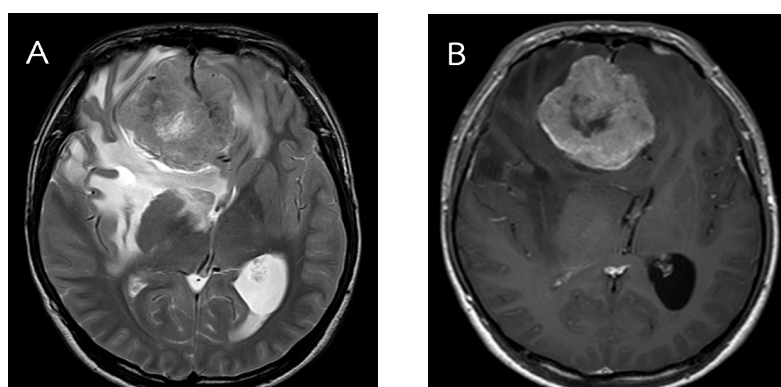


Figure 1. Axial T2- (A) and T1-weighted post-contrast (B) magnetic resonance images of a grade 2 meningioma showing heterogeneous enhancement of the tumor mass with central necrosis and peritumoral brain edema.

95% CI: 1.09–3.98, $p = 0.026$), necrosis or hemorrhage (OR = 4.28, 95% CI: 1.75–10.44, p value = 0.001), hyperostosis (OR = 0.28, 95% CI: 0.11–0.71, $p = 0.007$),

heterogeneous tumor enhancement (OR = 2.81, 95% CI: 1.46–5.42, $p = 0.002$), restricted diffusion (OR = 2.84, 95% CI: 1.24–6.51, $p = 0.014$), and brain edema (OR

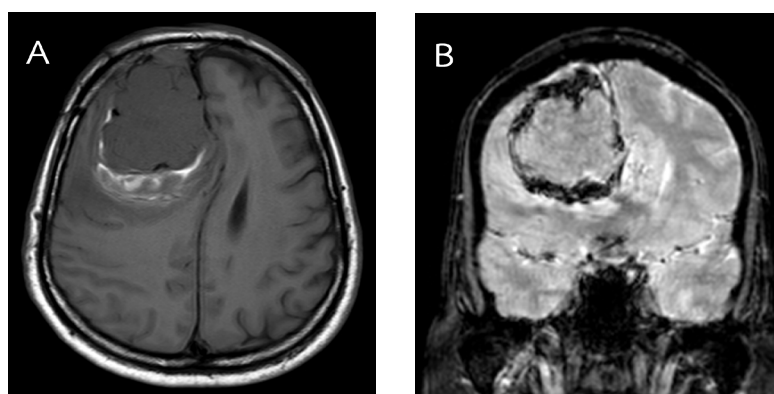


Figure 2. Axial T1-weighted (A) and coronal T2*GRE (B) magnetic resonance images of a grade 2 meningioma showing hemorrhagic component seen as a high signal intensity on T1-weighted image with blooming artifacts on T2*GRE

Table 2. Results of MRI Findings of the Patients

| Findings | Total (n = 210) | Low-Grade (n = 160) | High-Grade (n = 50) | p-value |
|-----------------------------------|-----------------|---------------------|---------------------|---------|
| Intratumoral signal heterogeneity | 85 (40.5) | 57 (35.6) | 28 (56.0) | 0.01 |
| Multifocality | 36 (17.1) | 27 (16.9) | 9 (18.0) | 0.845 |
| Midline shift | 97 (46.2) | 67 (41.9) | 30 (60.0) | 0.025 |
| Venous sinus invasion | 60 (28.6) | 48 (30.0) | 12 (24.0) | 0.412 |
| Necrosis or Hemorrhage | 23 (11.0) | 11 (6.9) | 12 (24.0) | 0.001 |
| Mass effect | 189 (90.0) | 143 (89.4) | 46 (92.0) | 0.589 |
| Cystic component | 19 (9.0) | 12 (7.5) | 7 (14.0) | 0.167 |
| Bone invasion | 52 (24.8) | 43 (26.9) | 9 (18.0) | 0.204 |
| Hyperostosis | 58 (27.6) | 52 (32.5) | 6 (12.0) | 0.005 |
| Spiculation | 1 (0.5) | 1 (0.6) | 0 (0.0) | 1 |
| Heterogeneous tumor enhancement | 67 (31.9) | 42 (26.3) | 25 (50.0) | 0.002 |
| Capsular enhancement | 6 (2.9) | 4 (2.5) | 2 (4.0) | 0.63 |
| Restricted diffusion | 28 (13.3) | 16 (10.0) | 12 (24.0) | 0.011 |
| Brain edema | 113 (53.8) | 77 (48.1) | 36 (72.0) | 0.003 |
| Unclear tumor-brain interface | 5 (2.4) | 2 (1.3) | 3 (6.0) | 0.09 |

Data are presented as number (%); The p value corresponds to Chi-square test or Fisher's exact test.

= 2.77, 95% CI: 1.39–5.53, $p = 0.004$) as significant predictors of high-grade meningioma ($p < 0.05$) (Table 3).

Meanwhile, multivariate analysis with Multiple Logistic regression analysis using factors determined to be significant during univariate analysis via a backward stepwise selection method with statistically significance set at 0.05 identified only three MRI features including necrosis or hemorrhage (adjusted OR = 2.94, 95% CI: 1.15–7.48, $p = 0.024$), hyperostosis (adjusted OR = 0.31, 95% CI: 0.12–0.79, $p = 0.014$), and brain edema (adjusted OR = 2.33, 95% CI: 1.13–4.81, $p = 0.022$) as significant independent predictors of high-grade meningioma after adjusting for confounders (Table 3).

Discussion

The current study showed that peritumoral brain edema was a significant predictor of high-grade meningioma following both univariate and multivariate analyses. The overall incidence of peritumoral brain edema was 53%, with low- and high-grade meningioma accounting for 48.1% and 72%, respectively. Meningiomas have the propensity to cause peritumoral brain edema despite being extracerebral in origin, benign, and slow-growing tumors. The exact mechanism by which peritumoral edema develops in meningiomas remains unclear. Nonetheless, several theories have been proposed to explain peritumoral edema in meningiomas, including tumoral compression of the adjacent parenchyma, vascular compression causing venous stasis, and the production of vascular endothelial growth factor (Hou et al., 2013; Toh et al., 2021).

Previous studies have found an association between peritumoral cerebral edema and meningioma histological grading. Hale et al., 2018 found that peritumoral edema was an independent predictor of higher-grade meningioma after adjusting for the presence of tumor necrosis and a draining vein. Certain studies have also observed a link between peritumoral brain edema and clinical outcomes

after surgery. Notably, Simis et al., 2008 found that peritumoral brain edema may be associated with the invasive potential of meningiomas and may play a role in the recurrence potential of the tumor, suggesting the need to consider its presence when mapping out strategies for the treatment of meningiomas. Qi et al., 2012 suggested that the presence of peritumoral brain edema might indicate a more difficult tumor resection, aggressive meningioma, and disruption of the arachnoid layer at the tumor–brain interface. Similarly, the current study concluded that imaging findings of peritumoral edema on preoperative MRI could potentially predict higher histological grading of meningioma and thus assist neurosurgeons in surgical planning and postoperative treatment of the patients.

Our findings showed that necrosis or hemorrhage on preoperative MRI was a significant predictor of high-grade meningioma following univariate and multivariate analyses. Among the 210 cases with intracranial meningioma who had available preoperative MR images, 23 (11%) exhibited imaging findings consisted with of necrosis or hemorrhage, among whom 11 (6.9%) and 12 (24%) had low- and high-grade meningioma, respectively. The mechanism by which necrosis develops in meningioma is assumed to be ischemia caused by feeding artery occlusion (Murai, 2007). The study done by Coroller et al., 2017 demonstrates that necrosis/hemorrhage features on MRI are associated with a high-grade tumor. Several prior studies have found a relationship between imaging findings of necrosis and the incidence of high-grade meningioma (Dietemann et al., 1982; Ayerbe et al., 1999; Hale et al., 2018). Notably, a study by Góes et al., 2018 showed that necrosis was a consistent factor for meningioma recurrence.

Spontaneous intratumoral hemorrhage is quite uncommon in patients with intracranial meningiomas. Although the underlying pathophysiological mechanisms for spontaneous intratumoral hemorrhage remain unclear,

Table 3: Univariate and Multivariate Analysis of Potential Predictors for High-Grade Meningioma

| Predictors | Univariable analysis | | | Multivariable analysis | | | Multivariable analysis | | |
|-----------------------------------|----------------------|----------------|---------|--------------------------------|---------------|---------|--------------------------------|---------------|---------|
| | OR ¹ | 95%CI | p-value | OR _{adj} ² | 95%CI | p-value | OR _{adj} ³ | 95%CI | p-value |
| Male sex | 2.84 | (1.33 - 6.06) | 0.007 | 2 | (0.87 - 4.59) | 0.103 | | | |
| Age ≥60 years | 1.43 | (0.70 - 2.89) | 0.327 | | | | | | |
| Location | | | | | | | | | |
| Skull base | 1 | Reference | | 1 | Reference | | | | |
| Parafalcine/parasagittal | 3.79 | (1.54 - 9.33) | 0.004 | 2.53 | (0.91 - 7.07) | 0.076 | | | |
| Convexity | 1.11 | (0.39 - 3.15) | 0.849 | 0.89 | (0.29 - 2.76) | 0.837 | | | |
| Posterior fossa | 1.29 | (0.47 - 3.52) | 0.617 | 1.25 | (0.40 - 3.90) | 0.697 | | | |
| Cavernous sinus | 1.02 | (0.20 - 5.22) | 0.986 | 1.71 | (0.30 - 9.86) | 0.55 | | | |
| Multicompartment | 0.68 | (0.21 - 2.21) | 0.518 | 1.07 | (0.30 - 3.83) | 0.919 | | | |
| MRI Findings | | | | | | | | | |
| Intratumoral signal heterogeneity | 2.3 | (1.21 - 4.39) | 0.011 | 0.7 | (0.23 - 2.11) | 0.526 | | | |
| Multifocality | 1.08 | (0.47 - 2.48) | 0.854 | | | | | | |
| Midline shift | 2.08 | (1.09 - 3.98) | 0.026 | 1.27 | (0.51 - 3.14) | 0.604 | | | |
| Venous sinus invasion | 0.74 | (0.35 - 1.53) | 0.413 | | | | | | |
| Necrosis or Hemorrhage | 4.28 | (1.75 - 10.44) | 0.001 | 2.23 | (0.73 - 6.83) | 0.159 | 2.94 | (1.15 - 7.48) | 0.024 |
| Mass effect | 1.37 | (0.44 - 4.27) | 0.59 | | | | | | |
| Cystic component | 2.01 | (0.74 - 5.42) | 0.168 | | | | | | |
| Bone invasion | 0.6 | (0.27 - 1.33) | 0.208 | | | | | | |
| Hyperostosis | 0.28 | (0.11 - 0.71) | 0.007 | 0.44 | (0.16 - 1.21) | 0.11 | 0.31 | (0.12 - 0.79) | 0.014 |
| Spiculation | - | - | NA | | | | | | |
| Heterogeneous tumor enhancement | 2.81 | (1.46 - 5.42) | 0.002 | 1.52 | (0.50 - 4.60) | 0.456 | | | |
| Capsular enhancement | 1.63 | (0.29 - 9.15) | 0.582 | | | | | | |
| Restricted diffusion | 2.84 | (1.24 - 6.51) | 0.014 | 1.54 | (0.58 - 4.09) | 0.39 | | | |
| Brain edema | 2.77 | (1.39 - 5.53) | 0.004 | 1.81 | (0.72 - 4.56) | 0.206 | 2.33 | (1.13 - 4.81) | 0.022 |
| Unclear tumor-brain interface | 5.01 | (0.81 - 30.88) | 0.082 | | | | | | |

Abbreviations: OR, Odds Ratio; OR_{adj}, Adjusted Odds Ratio; CI, confident interval; Variable was included in multivariate model due to have a p value < 0.050 in univariate analysis; ¹Crude Odds Ratio estimated by Binary Logistic regression; ²Adjusted Odds Ratio estimated by Multiple Logistic regression with enter method; ³Adjusted Odds Ratio estimated by Multiple Logistic regression with backward stepwise selection method

several hypotheses have been proposed, including weakening of the enlarged supply or draining vessels, granulation tissue from neovascularization, and meningeal invasion of the vessel wall (Bosnjak et al., 2005).

Previous studies have reported that angioblastic and malignant meningiomas have a higher potential for bleeding (Helle and Conley, 1980; Bruno et al., 2003). Meanwhile, Bosnjak et al., 2005 found that surgically treated meningiomas with hemorrhage lead to higher morbidity and mortality rates. The current study suggests that the presence of necrosis or hemorrhage on preoperative MRI of meningiomas should alert radiologists and surgeons regarding the possibility of a high-grade tumor.

Among our patients with meningioma, 58 (27.6%) exhibited hyperostosis on preoperative MRI, of whom 52 (32.5%) and 6 (12%) had low- and high-grade meningioma. This imaging finding had also been found to be a significant predictor in both univariate (adjusted OR = 0.28, 95% CI: 0.11–0.71, p = 0.007) and multivariate (adjusted OR = 0.31, 95% CI: 0.12–0.79, p = 0.014) analyses, implying its association with a decreased chance of high-grade meningioma. Although the cause of hyperostosis in meningioma remains controversial, several hypotheses have been proposed to explain its

development, including tumor invasion of the bone or the reactive process of the bone caused by the tumor (Terstegge et al., 1994; Pieper et al., 1999). A study by Goyal et al. 2012 found that a significant number of patients with radiological hyperostosis exhibited tumor invasion into the bone. The absence of hyperostosis, however, does not rule out tumor invasion. Consequently, although our study suggested that preoperative imaging findings of hyperostosis could be a predictor of low-grade meningioma, tumor invasion into the bone and subsequent risk of postoperative tumor recurrence in case of incomplete surgical resection can still occur.

Limitations

Our study has some limitations worth noting. Owing to its retrospective design, selection and information bias could not be avoided. Furthermore, our findings may not be generalizable to the entire population considering that our study population comprised of patients from a single tertiary hospital. Further prospective multicenter studies should yield more accurate results.

In conclusion, The current study found that preoperative MRI features of peritumoral brain edema and presence of necrosis/hemorrhage were significant predictive factors for high-grade intracranial meningioma, whereas

hyperostosis was a significant predictive factor for low-grade intracranial meningioma following multivariate analysis. The aforementioned findings could potentially assist in decision-making regarding the appropriate management and surgical approach in order to achieve the desired clinical outcomes. Further study of correlations between findings on preoperative MRI and tumor recurrence should offer additional clinical benefits.

Author Contribution Statement

All authors contributed to the study's conception and design. Material preparation, data collection, and analysis were performed by Kan Radeesri and Vitit Lekhavat. The first draft of the manuscript was written by Kan Radeesri, and all authors commented on previous versions of the manuscript. All authors have read and approved the final manuscript.

Acknowledgements

Funding

This study was funded by Navamindradhiraj University.

Employment

Department of Radiology, Faculty of Medicine Vajira Hospital, Navamindradhiraj University, Bangkok, Thailand.

Financial and non-financial interests

The authors have no relevant financial or non-financial interests to disclose.

Ethics approval

All procedures involving human participants were performed in accordance with the ethical standards of the institutional and/or national research committee and with the 1964 Helsinki Declaration and its later amendments or comparable ethical standards. The study was approved by the Bioethics Committee of Navamindradhiraj University (COA 173/63).

Consent to participate

The need for informed consent was waived because of the retrospective study design.

Consent for publication -

Data Availability

The datasets generated during and/or analyzed during the current study are available from the corresponding author on reasonable request.

References

Ayerbe J, Lobato RD, de la Cruz J, et al (1999). Risk factors predicting recurrence in patients operated on for intracranial meningioma. A multivariate analysis. *Acta Neurochir*, **141**, 921–32.

Bosnjak R, Derham C, Popovic M, et al (2005). Spontaneous intracranial meningioma bleeding: Clinicopathological features and outcome. *J Neurosurg*, **103**, 473–84.

Bruno MC, Santangelo M, Panagiotopoulos K, et al (2003). Bilateral chronic subdural hematoma associated with meningioma: Case report and review of the literature. *J Neurosurg Sci*, **47**, 215.

Budohoski KP, Clerkin J, Millward CP, et al (2018). Predictors of early progression of surgically treated atypical meningiomas. *Acta Neurochir*, **160**, 1813–22.

Claus EB, Bondy ML, Schildkraut JM, et al (2005). Epidemiology of intracranial meningioma. *Neurosurgery*, **57**, 1088–95.

Coroller TP, Bi WL, Huynh E, et al (2017). Radiographic prediction of meningioma grade by semantic and radiomic features. *PLoS One*, **12**, e0187908.

Dietmann JL, Heldt N, Burguet JL, et al (1982). CT findings in malignant meningiomas. *Neuroradiology*, **23**, 207–9.

Góes P, Santos BF, Suzuki FS, et al (2018). Necrosis is a consistent factor to recurrence of meningiomas: should it be a stand-alone grading criterion for grade 2 meningioma. *J Neurooncol*, **137**, 331–6.

Goldbrunner R, Minniti G, Preusser M, et al (2016). EANO guidelines for the diagnosis and treatment of meningiomas. *Lancet Oncol*, **17**, 383–91.

Goyal N, Kakkar A, Sarkar C, et al (2012). Does bony hyperostosis in intracranial meningioma signify tumor invasion? A radio-pathologic study. *Neurol India*, **60**, 50.

Gurkanlar D, Er U, Sanli M, et al (2005). Peritumoral brain edema in intracranial meningioma. *J Clin Neurosci*, **12**, 750–3.

Hale AT, Wang L, Strother MK, et al (2018). Differentiating meningioma grade by imaging features on magnetic resonance imaging. *J Clin Neurosci*, **48**, 71–5.

Helle TL, Conley FK (1980). Haemorrhage associated with meningioma: A case report and review of the literature. *J Neurol Neurosurg Psychiatry*, **43**, 725–9.

Hou J, Kshetry VR, Selman WR, et al (2013). Peritumoral brain edema in intracranial meningiomas: the emergence of vascular endothelial growth factor-directed therapy. *Neurosurg Focus*, **35**, E2.

Hsu CC, Pai CY, Kao HW, et al (2010). Do aggressive imaging features correlate with advanced histopathological grade in meningioma?. *J Clin Neurosci*, **17**, 584–7.

Hwang WL, Marciscano AE, Niemierko A, et al (2016). Imaging and extent of surgical resection predict risk of meningioma recurrence better than WHO histopathological grade. *Neurooncology*, **18**, 863–72.

Kawahara Y, Nakada M, Hayashi Y, et al (2012). Prediction of high-grade meningioma by preoperative MRI assessment. *J Neurooncol*, **108**, 147–52.

Lee KJ, Joo W, Rha H, et al (2008). Peritumoral brain edema in meningioma: correlations between magnetic resonance imaging, angiography, and pathology. *Surg Neurol*, **69**, 350–5.

Lin BJ, Chou KN, Kao HW, et al (2014). Correlation between magnetic resonance imaging grading and pathological grading in meningioma. *J Neurosurg*, **121**, 1201–8.

Louis DN, Perry A, Wesseling P, et al (2021). The 2021 WHO classification of tumors of the central nervous system: a summary. *Neurooncology*, **23**, 1231–51.

Murai N (2007). Three cases of fibrous meningioma with prominent central necrosis. *No Shinkei Geka*, **16**, 135–40.

Ogasawara C, Philbrick BD, Adamson DC (2021). Meningioma: A review of epidemiology, pathology, diagnosis, treatment, and future directions. *Biomedicine*, **9**, 319.

O'leary S, Adams WM, Parrish RW, Mukonoweshuro W (2007). Atypical imaging appearances of intracranial meningiomas. *Clin Radiol*, **62**, 10–7.

Pieper DR, Al-Mefty O, Hanada Y, et al (1999). Hyperostosis associated with meningioma of the cranial base: secondary

- changes or tumor invasion. *Neurosurgery*, **44**, 742-6.
- Qi ST, Liu Y, Pan J, et al (2012). A radiopathological classification of dural tail sign of meningiomas. *J Neurosurg*, **117**, 645-53.
- Rogers L, Barani I, Chamberlain M, et al (2015). Meningiomas: knowledge base, treatment outcomes, and uncertainties. A RANO review. *J Neurosurg*, **122**, 4-23.
- Simis A, de Aguiar PH, Leite CC, et al (2008). Peritumoral brain edema in benign meningiomas: correlation with clinical, radiologic, and surgical factors and possible role on recurrence. *Surg Neurol*, **70**, 471-7.
- Terstege K, Schörner W, Henkes H, et al (1994). Hyperostosis in meningiomas: MR findings in patients with recurrent meningioma of the sphenoid wings. *Am J Neuroradiol*, **15**, 555-60.
- Toh CH, Siow TY, Castillo M (2021). Peritumoral brain edema in meningiomas may be related to glymphatic dysfunction. *Front Neurosci*, **15**, 674898.
- Watts J, Box G, Galvin A, et al (2014). Magnetic resonance imaging of meningiomas: a pictorial review. *Insights Imaging*, **5**, 113-22.



This work is licensed under a Creative Commons Attribution-Non Commercial 4.0 International License.